Mesostructured Alumina Nanocomposites Synthesized via Reverse Microemulsion Route

Zhixiong You, Ioan Balint, and Ken-ichi Aika*
Department of Environmental Chemistry and Engineering, Interdisciplinary Graduate School of Science and Technology, Tokyo Institute of Technology, 4259 Nagatsuta-cho, Midori-ku, Yokohama 226-8502

(Received April 8, 2003; CL-030303)

Mesostructured alumina nanocomposites, with 10 nm pores after 500 °C calcination, have been synthesized by reverse-microemulsion route.

Supramolecule-templating route has been conventionally applied to the preparation of mesostructured alumina since the successful synthesis of MCM 41 by Mobil group in 1992.[1] Although mesostructured aluminas have been synthesized in the presence of ionic[2] and nonionic[3] template surfactants, these materials, unlike mesoporous silica, have limited ordered-pore structures; and their mesopores easily collapse because of the thin amorphous alumina walls, which trend to transform to α-polymorph when the materials are subjected to high temperatures.

Reverse microemulsion method is extensively used to synthesize uniform-sized metal and metallic oxide nanoparticles.[4] Herein we present for the first time that mesostructured aluminas, added with different amount of barium to promote the thermal stability of alumina nanoparticles (the molar ratios of Ba to Al are 0, 1/48, 1/24, and 1/12), can be prepared by reverse microemulsion route.

The key for successfully obtaining a high surface area mesostructured material is preparation of a stable and transparent reverse microemulsion. A typical reverse microemulsion system, used for synthesis of mesostructured alumina, consisting of 195 mL isooctane (2,2,4-trimethylpentane, Aldrich) as oil phase, 30 mL PEG 200 (polyethylene glycol 200, Wako) as surfactant, 75 mL distilled water, and appropriate amount of *n*-propanol acting as cosurfactant (for the mentioned composition, around 390 mL *n*-propanol was necessary for achieving a transparent microemulsion). The precursor solution was prepared by dissolving 2.764 g aluminum isopropoxide (Aldrich) and appropriate amount of barium isopropoxide (Aldrich) in 30 mL isooctane at about 80 °C. Since barium isopropoxide dissolves difficultly in isooctane, 20 mL of chelate agent (ethyl acetoacetate, Wako) was added to the precursor solution to accelerate the dissolution of barium isopropoxide. Subsequently, the precursor solution was added to the reverse microemulsion system and hydrolyzed at room temperature under stirring for ca. 20 h. Finally, the hydrolyzed mixture was divided into two portions: one portion was transferred into an autoclave and treated in it at 150 °C for 24 h; the other portion was directly subjected to the following recovery process. The recovery of the hydrothermally treated and non-hydrothermally treated samples was carried out by rotoevaporation of the solvents. The remained surfactant, which can not be removed in the rotoevaporation process, was decomposed at 500 °C for 2 h in argon first and then in air, respectively.

The textural properties of the resulting materials were characterized by nitrogen adsorption/desorption measurements, performed at −196 °C (BELSORP 28SA). The results are shown in Table 1 and Figure 1. By comparing the data listed in Table 1, it can be seen that hydrothermal treatment affects drastically the morphology of the resultant materials. The specific surface area of the hydrothermally treated samples is in the range of 260–320 m^2/g, larger than that of non-hydrothermally treated ones (70–250 m^2/g). Moreover, the pore volume of the hydrothermally treated materials is around 800 μL/g, about 2.5 times larger than that of non-hydrothermally treated samples.

The nitrogen adsorption/desorption isotherms of non-hydrothermally treated materials (Figure 1a) are of type IV, with hysteresis loops presence in relative pressure (P/P_0) range of 0.4-0.7. Type IV isotherms are generally characteristic for mesostructured materials. In addition, the shape of the hysteresis loops is H2 type according to the classification of IUPAC (1985).[5] The pore radius distributions of these materials, calculated by Dollimore–Heal (D–H) method[6] on the desorption branches, are narrow and sharp, centered at around 2 nm (Figure 1c and Table 1). The hydrothermally treated materials present also type IV isotherms as shown in Figure 1b, but their hysteresis loops shift to higher relative pressure range of 0.7–0.9, suggesting that the pore radius of these samples is larger (around 5 nm). This assumption is confirmed by the results of pore radius distributions (Figure 1d).

The crystalline structure, characterized by XRD, of the samples prepared without and with hydrothermal treatment is γ-alumina and γ-alumina plus small amount of barium carbonate, respectively. Hydrothermal treatment has been found to accelerate the crystallization of γ-alumina and the formation of barium carbonate, which is possibly produced by the reaction between $Ba(OH)_2$ and CO_2 resulted from the decomposition of the organic solvents in the autoclave.

The different morphology between the two kinds of samples was also observed by TEM. Figure 2 gives the representative TEM images. The non-hydrothermally treated samples mainly consist of nanoparticles having wormhole pores with a size of 4–6 nm, which is quite close to the average pore size (around 4 nm) shown in Figure 1c, and amorphous framework walls. The basal space of the lattice fringe structures, which can be also observed in Figure 2a, is smaller than the measured pore size (around 4 nm, Figure 1c). Thus, it seems that these lattice fringe structures have no significant contribution to the overall mesoporosity. In contrast, the hydrothermally treated samples exhibit discrete uniform rod-shaped nanoparticles with length of around

Table 1. Textural properties of Ba-doped aluminas, prepared with or without hydrothermal treatment, after calcination at 500 °C for 4 h

Ba/Al molar ratio	S_a[a], m^2/g		R_p[b], nm		V_p[c], μl/g	
	A[d]	N[e]	A	N	A	N
0	263	252	5.5	1.8	861	322
1/48	315	250	4.2	1.8	801	246
1/24	311	210	4.2	1.8	685	250
1/12	278	67	5.5	1.9	771	95

[a]S_a: BET specific surface area. [b]R_p: Average pore radius.
[c]V_p: Pore volume. [d]A: Hydrothermally-treated samples.
[e]N: Non-hydrothermally-treated samples.

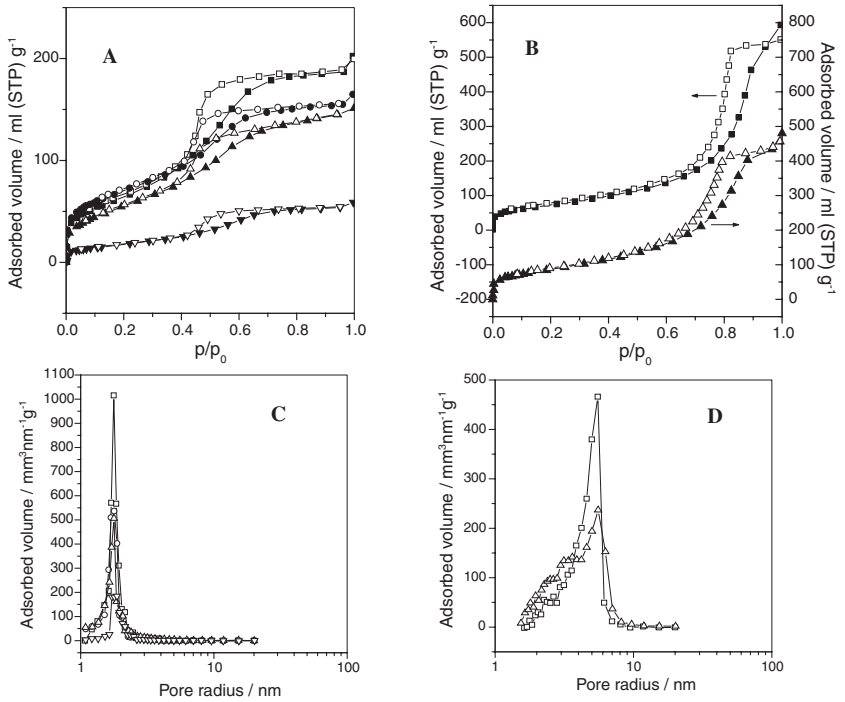

Figure 1. Nitrogen adsorption and desorption isotherms for Ba-doped aluminas synthesized without (A) and with (B) hydrothermal treatment. (In (B), the samples with Ba/Al molar ratio of 1/48 and 1/12 are not presented because they exhibit the same isotherms as the sample with Ba/Al molar ratio of 1/24.) The Pore radius distributions calculated by D–H method on the desorption branches for Ba-doped aluminas synthesized without (C) and with (D) hydrothermal treatment. (□ ■): Ba/Al molar ratio = 0, (○ ●): Ba/Al molar ratio = 1/48, (△ ▲): Ba/Al molar ratio = 1/24, and (▽ ▼): Ba/Al molar ratio = 1/12. In (A) and (B), closed symbols: adsorption branches and open symbols: desorption branches.

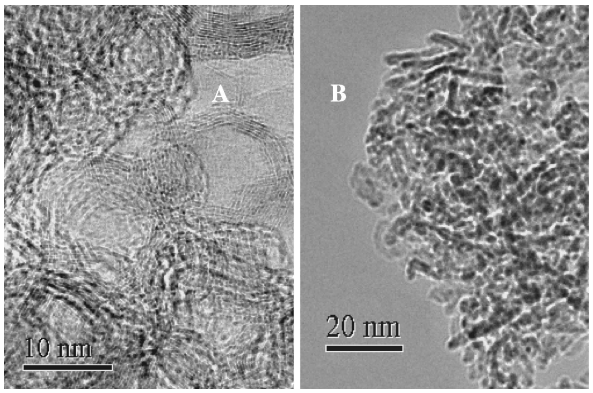

Figure 2. (A) TEM image for the non-hydrothermally treated sample containing Ba/Al molar ration of 1/12. (B) TEM image for the hydrothermally treated sample containing Ba/Al molar ratio of 1/24.

8 nm and width of about 3 nm (Figure 2b). Taking into account that the average pore size (pore diameter) is comparable with the size of particles, thus the mesopores of these materials must be generated from the voids among the uniform-sized nanoparticles. Additionally, since the distribution of the particle size is relatively narrow, the mesopores arose from the packing of these nanoparticles have comparable size with the particles and show narrow distribution as can be observed in Figure 1d.

This kind of interparticulate mesostructure, which is different from the mesoporosity presents in the matrix of the materials prepared by supramolecule templating route, depends on the uniformity of the nanoparticle size. Subsequently, as long as the nanoparticles are comparably sized, its mesostructure will be kept. For instance, when the hydrothermally treated sample, containing Ba/Al = 1/24, is calcined at 1100 °C for 24 h, it still shows type IV isotherm, but its hysteresis loop shifts to 0.8–0.95 relative pressure range. Its average pore size is around 20 nm, corresponding to the larger particle size (20 nm in length and 9 nm in width). By this way, a thermally stable mesostructured alumina nanocomposite, with surface area of about 145 m^2/g after calcination at 1100 °C for 24 h, has been synthesized successfully.[7]

References

1 a) C. T. Kresge, M. E. Lenowicz, W. J. Roth, J. C. Vartuli, and J. S. Beck, *Nature*, **359**, 710 (1992). b) J. S. Beck, J. C. Vartuli, W. J. Roth, M. E. Lenowicz, C. T. Kresge, K. D. Schmitt, C. T. Chu, D. H. Olson, E. W. Sheppard, S. B. McCullen, J. B. Higgins, and J. L. Schlenker, *J. Am. Chem. Soc.*, **114**, 10834 (1992).

2 a) F. Vaudry, S. Khodabandeh, and M. Davis, *Chem. Mater.*, **8**, 1451 (1996). b) M. Yada, H. Kitamura, M. Machida, and T. Kijima, *Langmuir*, **13**, 5252 (1997). c) W. S. Valenge, J. L. Guth, F. Kolenda, S. Lacombe, and Z. Gabelica, *Microporus Mesoporous Mater.*, **35**, 597 (2000).

3 a) S. A. Bagshaw and T. J. Pinnavaia, *Angew. Chem., Int. Ed. Engl.*, **35**, 1102 (1996). b) V. González-Peña, I. Díaz, C. Márquez-Alvarez, E. Sastre, and J. Pérez-Pariente, *Microporus Mesoporous Mater.*, **44-45**, 203 (2001). c) N. Cruise, K. Jansson, and K. Holmberg, *J. Colloid Interface Sci.*, **241**, 527 (2001). d) W. Zhang and T. J. Pinnavaia, *Chem. Commun.*, **1998**, 1185. e) Z. Zhang, R. W. Hicks, T. R. Pauly, and T. Pinnavaia, *J. Am. Chem. Soc.*, **124**, 1592 (2002).

4 a) M. J. Schwuger, K. Stickdom, and R. Schomäcker, *Chem. Rev.*, **95**, 849 (1995). b) J. Sjoblom, R. Lindberg, and S. E. Friberg, *Adv. Colloid Interface Sci.*, **95**, 125 (1996). c) A. Taleb, C. Petit, and M. P. Pileni, *Chem. Mater.*, **9**, 950 (1997). d) J. H. Adair, T. Li, T. Kido, K. Havey, J. Moon, J. Mecholsky, A. Morrone, D. R. Talham, M. H. Ludwig, and L. Wang, *Mater. Sci. Eng., R*, **23**, 139 (1998). e) M. Lade, H. Mays, J. Schmidt, R. Willumeit, and R. Schomäcker, *Colloids Surf., A*, **163**, 3 (2000). f) C. B. Murray, C. R. Kagen, and M. G. Bawendi, *Annu. Rev. Mater. Sci.*, **30**, 545 (2000). g) K. C. Song and J. H. Kim, *Powder Technol.*, **107**, 268 (2000). h) A. J. Zarur and J. Y. Ying, *Nature*, **403**, 65 (2000).

5 F. Rouquerol, J. Rouquerol, and K. Sing, "Adsorption by Powders and Porous Solids: Principles, Methodology and Applications," Academic Press, London (1999), Chap. 7, p 19.

6 D. Dollimore and G. R. Heal, *J. Appl. Chem.*, **14**, 109 (1964).

7 I. Balint, Z. You, and K. Aika, *Phys. Chem. Chem. Phys.*, **4**, 2501 (2002).

Published on the web (Advance View) June 24, 2003; DOI 10.1246/cl.2003.630